

# High-Specificity Thiocrown Ether Reagents for Silver(I) over Bivalent Mercury and Lead. Thermodynamic and $^{13}\text{C}$ NMR Relaxation Time Studies

G. Wu,<sup>†</sup> W. Jiang, J. D. Lamb, J. S. Bradshaw, and R. M. Izatt\*

Contribution from the Department of Chemistry, Brigham Young University, Provo, Utah 84602.  
Received January 18, 1991

**Abstract:** Log  $K$ ,  $\Delta H$ , and  $\Delta S$  values for the interactions of  $\text{Ag}^+$ ,  $\text{Hg}^{2+}$ , and  $\text{Pb}^{2+}$  with several thiocrown ether ligands were determined in aqueous solution by potentiometry and calorimetry.  $^{13}\text{C}$  NMR spin-lattice relaxation times ( $T_1$ ) and chemical shifts ( $\delta$ ) have been determined for pyridonothia-18-crown-6 (PT18C6) in the absence and presence of  $\text{Ag}^+$ ,  $\text{Hg}^{2+}$ , and  $\text{Pb}^{2+}$ . A large enhancement of selectivity by PT18C6 for  $\text{Ag}^+$  over  $\text{Hg}^{2+}$  and  $\text{Pb}^{2+}$  was found. The interactions of thiocrown ether ligands with the metal ions studied were found to be enthalpy driven. The entropy changes were unfavorable in all cases. The  $T_1$  and  $\delta$  measurements for PT18C6 interaction with  $\text{Ag}^+$  and  $\text{Hg}^{2+}$  in conjunction with the corresponding thermodynamic data provide a detailed microscopic picture of the macrocycle-metal ion interactions. Both  $\text{Ag}^+$  and  $\text{Hg}^{2+}$  interact strongly with the sulfur portion of PT18C6, but  $\text{Ag}^+$  interacts much more strongly than  $\text{Hg}^{2+}$  with the pyridone portion of the ligand. The influence of preorganization of the binding sites in the macrocycle on binding strength and selectivity was examined. A successful reversal of the common selectivity order of  $\text{Hg}^{2+}$  over  $\text{Ag}^+$  was accomplished by the insertion of a pyridone binding subunit in the thiocrown ether ligand system.

## Introduction

Highly selective reagents for metal ions are of great importance to broad areas of analytical and separation chemistry. The ability to design and synthesize such reagents was greatly aided by the early work of Pedersen<sup>1</sup> involving the preparation and demonstrated cation selectivity behavior of crown ethers. Ligand design principles such as size-match selectivity; achievement of coordination saturation of the metal ion; and the number, type, and location of macrocycle donor atoms have been applied with considerable success to achieve the selective complexation<sup>2</sup> of alkali and alkaline earth metal ions. The design of ligands for the selective complexation of transition-metal and post-transition-metal ions has received less attention. However, excellent examples of successful ligand design for these metal ions have been reported.<sup>3-5</sup> Cyclization reactions carried out without regard for these design principles can result in ligands with divergent donor atoms and groups that have a poor coordination geometry<sup>6</sup> for complexed metal ions.

The term "dislocation discrimination" has been used<sup>4</sup> to describe the variation from normal selectivity orders for several first-row transition-metal ions with use of appropriately designed macrocycles.<sup>5</sup> The selectivity of  $\text{Ag}^+$  over  $\text{Pb}^{2+}$  is found with  $\text{A}_2\text{18C6}$  and  $\text{T}_2\text{18C6}$ .<sup>2</sup> It is of interest to learn whether or not the introduction of other donor atoms and/or groups will enhance this selectivity. Hancock<sup>3</sup> has demonstrated selectivity enhancement for  $\text{Cu}^{2+}$  and  $\text{Zn}^{2+}$  over  $\text{Pb}^{2+}$  by changing the number, type, and location of macrocycle donor groups. However, the reversal of the normal selectivity order of  $\text{Hg}^{2+}$  over  $\text{Ag}^+$  is rare and is considered more difficult to achieve. This difficulty results from the greater affinity of  $\text{Hg}^{2+}$  for most "soft", "borderline", and even "hard" donor atoms and groups and the very similar radii<sup>7</sup> of  $\text{Ag}^+$  and  $\text{Hg}^{2+}$  which precludes the use of macrocycle size-match selectivity to attain the desired discrimination.

In this study, we demonstrate that the different coordination geometries of  $\text{Ag}^+$  and  $\text{Hg}^{2+}$  together with their relative affinities for various donor atoms or groups can be used to generate a reversal of the normal  $\text{Hg}^{2+}$  over  $\text{Ag}^+$  selectivity order.<sup>2</sup> The compounds studied are given in Figure 1. Three different techniques are used to investigate the metal ion-ligand binding. Equilibrium constants ( $K$ ) for metal-ligand interaction were determined either potentiometrically or calorimetrically. Corresponding enthalpy ( $\Delta H$ ) and entropy ( $\Delta S$ ) change values were

determined calorimetrically.  $^{13}\text{C}$  NMR relaxation time ( $T_1$ ) and chemical shift ( $\delta$ ) measurements were performed to provide information on ligand conformation, binding strength, and binding dynamics in solution. The  $^{13}\text{C}$  NMR technique offers a convenient means to identify the metal-binding contributions of specific binding sites in different portions of a multidentate ligand system. The  $T_1$  and  $\delta$  values are necessary to explain the macroscopic thermodynamic quantities and binding selectivities in a microscopic sense and, thus, to provide a rational ligand design strategy for heavy metals.

## Experimental Section

**Materials.** Metal salts (Alfa), 1,4- $\text{T}_2\text{18C6}$  (Parish), and 1,10- $\text{T}_2\text{18C6}$  (Parish) were purchased and used without further purification. The pyridonothia-18-crown-6 (PT18C6) was prepared as described previously.<sup>8</sup> Spectral grade  $\text{D}_2\text{O}$  (99.7%, Merck) and  $\text{CH}_3\text{OH}$  (Aldrich) were used. Deionized distilled water was used for the potentiometric and calorimetric studies.

**Emf Measurements.** The semimicro potentiometric titrations were carried out in a sealed, thermostated vessel (6 mL,  $25 \pm 0.1$  °C) under a  $\text{CO}_2$ -free nitrogen atmosphere with use of a semiautomatic titrator (Metrohm) or a fully automatic potentiometric titration unit of our own design.  $\text{CO}_2$ -free standard 0.1 M KOH was used as the titrant. The hydrogen ion concentration was measured with an Orion-Ross double junction semimicro combination glass electrode and an Orion 701A potentiometer adjusted with standard  $\text{HNO}_3$  and KOH solutions to read emf values directly.

Standard electrode potentials,  $E^\circ$  (371.6 mV), and the ion product of water,  $\text{p}K_{\text{w}}$  (13.685), were determined by titrating a  $\text{HNO}_3$  solution (3-5 mL) containing  $\text{HNO}_3$  with standard KOH solution. The value, 13.685, is required to fit the experimental data. This value is somewhat lower than that, 13.787, determined in 0.11 M KCl at 25 °C.<sup>9</sup> The  $K$  values for ligand protonation and for metal ion-ligand interaction were com-

\* Author to whom correspondence should be addressed.

<sup>†</sup> Present Address: Chemistry Division, Oak Ridge National Laboratory, Oak Ridge, TN 37831.

- (1) Pedersen, C. J. *J. Am. Chem. Soc.* **1967**, *89*, 7017-7036.
- (2) Izatt, R. M.; Bradshaw, J. S.; Nielsen, S. A.; Lamb, J. D.; Christensen, J. J.; Sen, D. *Chem. Rev.* **1985**, *85*, 271-339. Izatt, R. M.; Pawlak, K.; Bradshaw, J. S.; Bruening, R. L. *Chem. Rev.* In press.
- (3) Hancock, R. D. *Pure Appl. Chem.* **1986**, *58*, 1445-1452.
- (4) Adam, K. R.; Ansell, C. W. G.; Dancy, K. P.; Drummond, L. A.; Leong, A. J.; Lindoy, L. F.; Tasker, P. A. *J. Chem. Soc., Chem. Commun.* **1986**, 1011-1012.
- (5) Lindoy, L. F. *Pure Appl. Chem.* **1989**, *61*, 1575-1580.
- (6) Abstracts, *XV International Symposium on Macrocyclic Chemistry*, Odessa, USSR, September 2-7, 1990.
- (7) Marcus, Y. *Chem. Rev.* **1988**, *88*, 1475-1498.
- (8) Bradshaw, J. S.; Nakatsuji, Y.; Huszthy, P.; Wilson, B. E.; Dalley, N. K.; Izatt, R. M. *J. Heterocycl. Chem.* **1986**, *23*, 353-360.
- (9) Harned, H. S.; Hamer, W. J. *J. Am. Chem. Soc.* **1933**, *55*, 2194-2206.

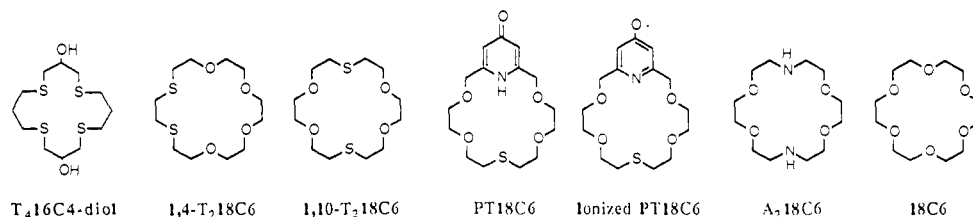


Figure 1. Structural formulas of macrocycles studied.

puted from data obtained by titrating acidified ligand solutions (3–5 mL) with KOH in the absence and presence, respectively, of the metal ion. A minimum of two runs was made for each system. Emf values were reproducible within  $\pm 0.3$  mV.

All calculations concerning the calibration of the electronic system, the purity of the ligands, and the  $pK_{i,p}$  value were performed with the program SUPERQUAD,<sup>10</sup> which refines the parameters of an acid–base potentiometric titration. Protonation and ionization constants for PT18C6 and metal ion binding constants for PT18C6 with  $\text{Ag}^+$  and  $\text{Hg}^{2+}$  were calculated from potentiometric titration data. No precipitates were found in the entire titration range from +250 to –290 mV in the cases of  $\text{Ag}^+$  and  $\text{Hg}^{2+}$ .

**Calorimetric Measurements.** Procedures used to determine  $\log K$ ,  $\Delta H$ , and  $\Delta S$  values by direct and competitive calorimetric titration techniques have been described.<sup>11</sup> In the case of the interaction of  $\text{Ag}^+$  with 1,10- $T_2$ 18C6, the  $\log K$  value is larger than 5. Hence, a competitive procedure involving the titration of 1,10- $T_2$ 18C6 against  $\text{Ag}^+$ -18C6<sup>2</sup> was used to determine  $\log K$  for  $\text{Ag}^+$ -1,10- $T_2$ 18C6 interaction.

**$T_1$  Measurements.** NMR samples consisted of 0.5 mL of solution in 5 mm o.d. tubes. All glassware was washed with 0.01 M EDTA solution to remove paramagnetic metal impurities. Relaxation time experiments were performed in 0.4–0.5 M pyridone ligand solutions in a mixed solvent of  $\text{CH}_3\text{OH}/\text{D}_2\text{O}$  (50/50 wt %). Stoichiometric amounts of ligand and metal nitrate salts were used for the complexation studies. For the metal–ligand interactions involving  $\text{Ag}^+$  and  $\text{Hg}^{2+}$ , the fraction found in the complexed form is essentially 100% since  $\log K$  values are  $\geq 4$  (Table I). Therefore, the possible error in the  $T_1$  values introduced by incomplete complex formation is comparable to the observed standard deviation of the measurements.

$^{13}\text{C}$  NMR spectra were obtained on a Varian 50-MHz (200-MHz  $^1\text{H}$ ) Gemini spectrometer. Calibration of the  $90^\circ/180^\circ$  pulse width was done by monitoring signal amplitude as a function of pulse length for methanol which yielded a high signal-to-noise ratio after only one pulse. Meantime, the carrier frequency was set close to that of the methanol peak. For the pulse width calibration, a full relaxation delay of 80 s ( $>5T_1$ ) for methanol was used, allowing complete relaxation between each trial. Pulse width was checked routinely because of a multiuser, multinuclei environment. Relaxation times were measured under a proton-noise-decoupling condition by an inversion–recovery technique. The recovery delays were made at least five times longer than the longest relaxation time among the corresponding carbon atoms in each experiment. Two kinds of pulse sequence and of carrier frequency were used to determine  $T_1$  for different types of carbon atoms. A delay of 80 s was used for the methanol. A delay of 4 s was used for methylene carbon atoms. It was our experience that in each experiment, the distribution of the  $t$  values is more important than the number of  $t$  values in determining the precision of the  $T_1$  values. The strategy for selecting  $t$  values varies according to the range of  $T_1$  values to be measured, and one long delay ( $t = \text{ca. } 5T_1$ ) was always used in the array of delays. At least nine points were included for each  $T_1$  calculation. All spectra were recorded at  $30 \pm 0.1^\circ\text{C}$ , and each run took 8–10 h. The determination of  $T_1$  values was made directly by the spectrometer computer with use of a direct least-squares fitting to a multiparameter exponential equation.

The experimental parameters and conditions were nearly identical among different batches of samples. At least two runs were made for each system. The standard errors were ca. 5% based on the values from all runs. Although absolute  $T_1$  values are not critical in this study, the  $T_1$  value of the  $\text{CH}_3\text{OH}$  resonance was still used as an internal standard for both  $T_1$  and  $\delta$  measurements. The  $T_1$  values obtained ranged from 12.6 to 13.2 s, in excellent agreement with literature values.<sup>12</sup> The 50 wt % mixed solvent system ( $\text{CH}_3\text{OH}/\text{D}_2\text{O}$ ) was necessary in order to

Table I.  $\log K$  Values<sup>a</sup> for the Interactions of  $\text{H}^+$ ,  $\text{Ag}^+$ ,  $\text{Hg}^{2+}$ , and  $\text{Pb}^{2+}$  with Several 18-Crown-6 Macrocyces in Aqueous Solution

cation	1,10- $T_2$ 18C6	PT18C6 <sup>-</sup>	PT18C6	$A_2$ 18C6	18C6
$\text{H}^+$		10.13 (1)	3.03 (1)		
$\text{Ag}^+$	5.27 (5)	9.44 (1)	5.36 (1)	7.8 <sup>c</sup>	1.60 <sup>c</sup>
$\text{Hg}^{2+}$	19.5 <sup>b</sup>	9.75 (1)	3.99 (1)	17.8 <sup>c</sup>	2.42 <sup>c</sup>
$\text{Pb}^{2+}$	3.31 (5)		<1	6.9 <sup>c</sup>	4.27 <sup>c</sup>

<sup>a</sup> Valid at  $\mu = 0.1$  ( $\text{HNO}_3$  or  $\text{KNO}_3$ ) and  $T = 25^\circ\text{C}$ ; uncertainties are indicated in parentheses. The 1,10- $T_2$ 18C6  $K$  values were determined from calorimetric data; the remaining  $K$  values were determined from potentiometric data. <sup>b</sup> Reference 13. <sup>c</sup> Reference 2.

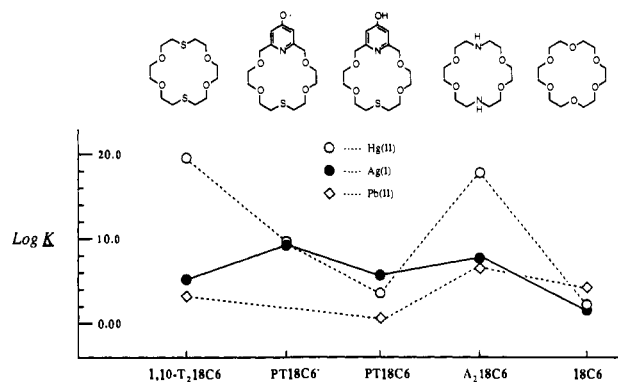


Figure 2. Plot of  $\log K$  for  $\text{Ag}^+$ ,  $\text{Hg}^{2+}$ , and  $\text{Pb}^{2+}$ –macrocycle interaction vs macrocycle arranged in the order of decreasing overall donor atom softness.

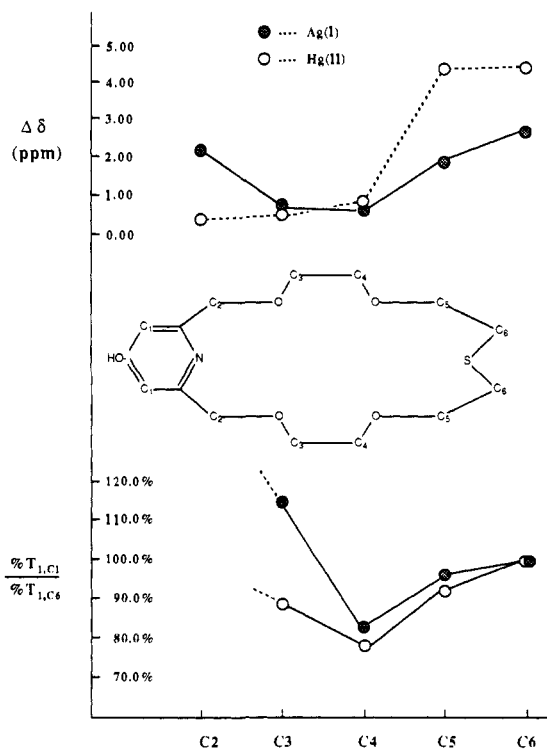


Figure 3. Chemical shift and relative  $T_1$  percentage drop curves for various carbons in PT18C6 complexes with  $\text{Ag}^+$  and  $\text{Hg}^{2+}$ .

(10) Gans, P.; Sebatini, A.; Vacca, A. *J. Chem. Soc., Dalton Trans.* **1985**, 1195–1200.

(11) Izatt, R. M.; Wu, G. *Thermochim. Acta* **1989**, *154*, 161–166.

(12) Abraham, R. J.; Loftus, F. *Proton and Carbon-13 NMR Spectroscopy*; Heyden: London, 1979.

**Table II.**  $\log K$ ,  $\Delta H$ , and  $\Delta S$  Values<sup>a</sup> for the Interactions of  $\text{Ag}^+$  with Several Macrocyclic Ligands in Aqueous Solution

ligand	T <sub>4</sub> 14C4-diol	1,4-T <sub>2</sub> 18C6	1,10-T <sub>2</sub> 18C6	PT18C6	PT18C6 <sup>-</sup>	A <sub>2</sub> 18C6	18C6
$\log K$	2.67 (5)	3.05 (5)	5.27 (5)	5.36 (1)	9.44 (1)	7.8 <sup>b</sup>	1.6 <sup>b</sup>
$\Delta H$ , kJ/mol	-47.0 (4)	-65.7 (4)	-75.0 (4)			-38.3 <sup>b</sup>	-9.1 <sup>b</sup>
$\Delta S$ , J/(K mol) <sup>-1</sup>	-107	-163	-141			21 <sup>b</sup>	-1.7 <sup>b</sup>

<sup>a</sup> Valid at  $\mu = 0.1$  ( $\text{HNO}_3$  or  $\text{KNO}_3$ ) and  $T = 25$  °C. All  $K$  values were determined from calorimetric data, except those for PT18C6 and PT18C6<sup>-</sup> which were determined from potentiometric data. Uncertainties are indicated in parentheses. <sup>b</sup> Reference 1.

**Table III.** <sup>13</sup>C NMR Relaxation Times ( $T_1$ )<sup>a</sup> and Chemical Shifts ( $\delta$ )<sup>a</sup> for PT18C6 and Its  $\text{Ag}^+$  and  $\text{Hg}^{2+}$  Complexes in 50% (wt) MeOH/D<sub>2</sub>O at 30 °C

species	parameter	C-1	C-2	C-3 <sup>b</sup>	C-4 <sup>b</sup>	C-5 <sup>b</sup>	C-6 <sup>b</sup>
PT18C6	$T_1$ , s			0.734	0.605	0.691	0.641
	$\delta$ , ppm	117.07 <sup>c</sup>	73.08	72.93	72.47	71.60	34.21
$\text{Ag}^+$ complex	$T_1$ (% $T_1$ )			0.412 (43.9) <sup>d</sup>	0.414 (31.6) <sup>d</sup>	0.433 (37.3) <sup>d</sup>	0.374 (38.5) <sup>d</sup>
	% $T_{1C_i}$ / % $T_{1C_6}$			114.0	82.1	96.8	100
	$\delta$ , ppm	113.90 <sup>c</sup>	75.22	72.21	71.76	69.65	36.85
$\text{Hg}^{2+}$ complex	$ \Delta\delta $ , ppm	3.17	2.14	0.72	0.71	1.95	2.64
	$T_1$ (% $T_1$ )			0.431 (41.3) <sup>d</sup>	0.385 (36.4) <sup>d</sup>	0.393 (43.1) <sup>d</sup>	0.341 (46.8) <sup>d</sup>
	% $T_{1C_i}$ / % $T_{1C_6}$			88.2	77.8	92.1	100
	$\delta$ , ppm	115.32 <sup>c</sup>	72.69	72.38	71.65	67.30	38.51
	$ \Delta\delta $ , ppm	1.75	0.39	0.55	0.82	4.30	4.31

<sup>a</sup>  $\text{CH}_3\text{OH}$  was used as an internal standard for both  $T_1$  and  $\delta$  measurements;  $T_1$  values are given in seconds; resonance peaks were measured with a precision better than 0.01 ppm. <sup>b</sup> A single carrier frequency was used for the indicated carbon atoms.  $T_1$  values were measured for C<sub>3</sub>, C<sub>4</sub>, C<sub>5</sub>, and C<sub>6</sub> only because of the selected carrier frequency used. In C-*i*, *i* is a running integer from 1 to 6. <sup>c</sup> These values might not be directly comparable because of the unknown percent contributions to  $\delta$  of the tautomerization of PT18C6 and the metal binding. <sup>d</sup> Values in parentheses are the percentage decreases in the  $T_1$  value when the ligand is complexed by the indicated cation.

obtain sufficient solubilities of both uncomplexed and complexed macrocyclic ligands.

## Results and Discussion

$\log K$  values for the interactions of  $\text{H}^+$ ,  $\text{Ag}^+$ ,  $\text{Hg}^{2+}$ , and  $\text{Pb}^{2+}$  with the macrocyclic ligands studied are given in Table I.  $\log K$ ,  $\Delta H$ , and  $\Delta S$  values for the interactions of  $\text{Ag}^+$  with several macrocycles are given in Table II. A reversal of the common order of selectivity of  $\text{Hg}^{2+}$  over  $\text{Ag}^+$  is shown in Figure 2 for PT18C6. <sup>13</sup>C NMR  $T_1$  and  $\delta$  values for the ligand PT18C6 and its  $\text{Ag}^+$  and  $\text{Hg}^{2+}$  complexes, determined at 50.3 MHz in a 50 wt %  $\text{CH}_3\text{OH}$ -D<sub>2</sub>O solvent, are reported in Table III and Figure 3. Individual carbon spectral assignments were made on the basis of the  $T_1$  and  $\delta$  values. The difference between the  $T_1$  values before and after interaction with the designated cations is expressed as the percent by which the values decreased. The cation binding characteristics of the macrocyclic ligands studied are now discussed.

**Effect of Combinations of Different Donor Groups in 18-Crown-6 on Ligand Complexing Ability.** In contrast to the extensive investigation of thiaether-copper(II) coordination chemistry, few studies have been reported of thiaether complexes of  $\text{Ag}^+$  and other thiophilic metal ions.<sup>2,13</sup>  $\text{Ag}^+$  has affinity for both thiaether and oxa ether donor groups, although cation-dipole interactions predominate in  $\text{Ag}^+$ -oxygen interactions.<sup>14</sup> An optimum combination of different types of "hard", "soft", and "borderline" ligand donor groups is required for  $\text{Ag}^+$  to reach a maximum selectivity over other thiophilic metal ions such as  $\text{Cu}^{2+}$ ,  $\text{Hg}^{2+}$ , and  $\text{Pb}^{2+}$ . We hypothesized that it might be possible to combine different types of ligand donor atoms in such a manner as to lead to enhanced binding of  $\text{Ag}^+$  over other transition-metal and post-transition-metal ions. In addition to the type of donor atoms, their placement in the ligand is expected to be important. For example, 1,10-substituted 18C6 ligands were considered to be the best to meet the linear coordination geometry of  $\text{Ag}^+$ .

Five different 18C6-type ligands were studied. As shown in Table II, the affinity of A<sub>2</sub>18C6 for  $\text{Ag}^+$  is much larger than that of any of the neutral thiaether macrocycles, indicating that  $\text{Ag}^+$  is in the class of metal ions which prefers borderline ligand donor groups. The large drop in  $\log K$  in going from 1,10-T<sub>2</sub>18C6 to 1,4-T<sub>2</sub>18C6 (Table II) results from a combination of less favorable changes in both  $\Delta H$  and  $\Delta S$  in the case of the latter compound.

The major effects seem likely to be the unfavorable orbital overlapping affecting  $\Delta H$  and the unfavorable strain energy affecting  $\Delta S$  in the 1,4-T<sub>2</sub>18C6 ligand.

One of the most interesting points evident in the thermodynamic properties in Table II is that the thiaether complexation is enthalpy driven with unfavorable entropy changes in all cases. The much larger ( $-\Delta S$ ) terms of the 1:1 reactions of  $\text{Ag}^+$  with the two T<sub>2</sub>18C6 ligands compared to those of the corresponding reactions with 18C6 and A<sub>2</sub>18C6 result from the replacement of oxygen or nitrogen by sulfur. These large unfavorable entropy changes are probably associated with the significant conformational changes (from exo to endo) of the thiaether moieties expected upon complexation<sup>14</sup> and the significantly smaller degree of dehydration required for sulfur vs oxygen/nitrogen donor atoms.

**Creation of an Unusual Selectivity Order ( $\text{Ag}^+$  over  $\text{Hg}^{2+}$ ) by Incorporating a Pyridone Binding Subunit in the Macrocyclic.** A characteristic feature of the reactions studied is that the binding strength of  $\text{Hg}^{2+}$  with all ligands except PT18C6 is superior to that of  $\text{Ag}^+$  (Figure 2). A large drop in the stability of  $\text{Hg}^{2+}$  complexes occurs upon replacement of one S of T<sub>2</sub>18C6 by the pyridone moiety. However, little change in the stability of  $\text{Ag}^+$  complexes occurs, indicating that pyridone derivatives of 18C6 may be superior ligands to discriminate  $\text{Ag}^+$  from other strong thiophilic metal ions.

The  $\delta$  values resulting from complexation (Figure 3) clearly indicate that  $\text{Hg}^{2+}$  lacks affinity for the pyridone-binding subunit. However,  $\text{Ag}^+$  binds strongly with the pyridone group, as illustrated by the large shift (3.17 ppm) of C-1 (Table III). Also, the downshift of C-2 in the  $\text{Ag}^+$ -PT18C6 complex indicates a lowered ring current in the pyridone moiety as electrons are donated to  $\text{Ag}^+$  through the pyridone nitrogen. The large anisotropic shifts of C-6 in  $\text{Ag}^+$ -PT18C6<sup>+</sup> and  $\text{Hg}^+$ -PT18C6<sup>2+</sup> are consistent with the expectation of large affinities of the thiaether group with both  $\text{Hg}^{2+}$  and  $\text{Ag}^+$ . As we proceed from C-5 to C-2, the absolute isotropic carbon shifts decrease in both complexes from C-5 to C-4. However, the absolute shift for the  $\text{Ag}^+$ -PT18C6 complex increases from C-3 to C-2, indicating strong interaction of  $\text{Ag}^+$  with the pyridone portion of the ligand. Therefore,  $\text{Ag}^+$  appears to bind covalently to both sulfur and pyridone nitrogen. This linear coordination brings the  $\text{Ag}^+$  into the macrocycle cavity making cation-dipole interaction with the ether oxygen atoms possible.<sup>14</sup> On the other hand,  $\text{Hg}^{2+}$  binds tightly with only the

(13) Izatt, R. M.; Wu, G.; Jiang, W.; Dalley, N. K. *Inorg. Chem.* 1990, 29, 3828-3832.

(14) Wu, G.; Izatt, R. M.; Jiang, W.; Dalley, N. K. *Inorg. Chim. Acta.* In preparation.

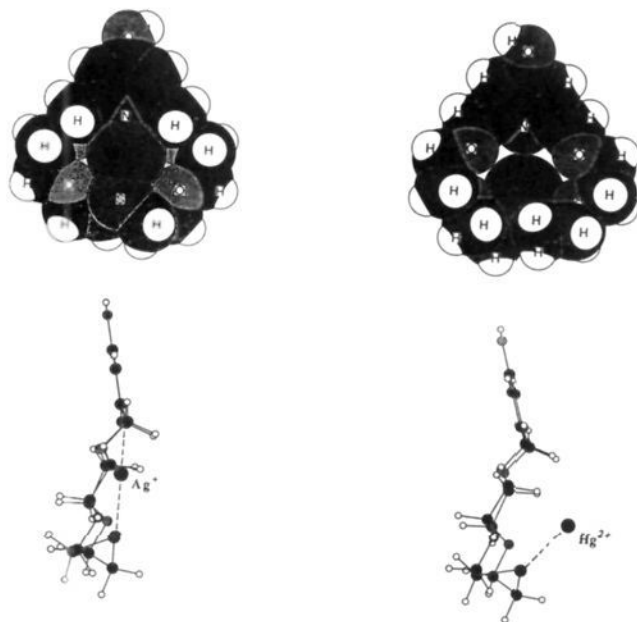


**Figure 4.** Possible coordination patterns of PT18C6 complexes of  $\text{Ag}^+$  and  $\text{Hg}^{2+}$  in solution. The patterns represented do not necessarily correspond to the exact structure of each complex in solution.

thiaether fragment, leaving the pyridone portion of the ligand free to move about.

The  $^{13}\text{C}$  relaxation times further support the structural analysis described above. It is well-known that the  $T_1$  values for any given molecule depend upon molecular mobility (tumbling) as determined by the internal degrees of freedom of the molecule.<sup>15</sup> The measurement of  $T_1$  values for each resolvable resonance can lead to estimates of relative mobilities of the different portions of the macrocyclic ring framework in solution. Metal ion complexation results in an increase in the effective molecular weight. Thus, there is less freedom for the complex to tumble resulting in an increase in correlation time, or a decrease in  $T_1$ . Instead of making direct comparison of the  $T_1$  values of different molecular weight cation complexes as was done by Echegoyen et al.,<sup>16</sup> we compared the  $T_1$  values of the uncomplexed ligand with those of the complexed ligand and the  $T_1$  values of the carbon atoms in different portions of the same complexed molecule. When PT18C6 is bound by either  $\text{Hg}^{2+}$  or  $\text{Ag}^+$ , a dramatic decrease in the mobility of all carbons is observed (Table III). The relaxation time of C-6 is

reduced to a large degree in both the  $\text{Hg}^{2+}$  and  $\text{Ag}^+$  complexes, which is consistent with the thiophilicity of  $\text{Hg}^{2+}$  and  $\text{Ag}^+$  ions.

Since the molecular weight of PT18C6 increases 30% more on complexation with  $\text{Hg}^{2+}$  than with  $\text{Ag}^+$ , a direct comparison of the percentage drops of  $T_1$  between the two complexes may be misleading. Instead, comparison of intramolecular  $T_1$  values led to an interesting feature of PT18C6 complexation with  $\text{Ag}^+$  and  $\text{Hg}^{2+}$ . The C-6 carbon was used as a reference state for intramolecular  $T_1$  comparison, considering that both  $\text{Hg}^{2+}$  and  $\text{Ag}^+$  bind tightly to the thiaether group. As we proceed from C-6 to C-3 (Figure 3), the ratio of the percentage decrease of  $T_1$  for a given carbon relative to that for C-6 ( $\% T_{1,C-i} / \% T_{1,C-6}$ ) becomes smaller in the case of  $\text{Hg}^{2+}$ -PT18C6 with a small increase between C-4 and C-3. In the case of  $\text{Ag}^+$ , the ratio also decreases from C-6 to C-4, but increases significantly between C-4 and C-3, indicating a tighter binding of  $\text{Ag}^+$  with the pyridone portion of the ligand. Figure 3 is constructed with use of the underlined values in Table III. In this figure, both the chemical shift and relative  $T_1$  curves show a very similar pattern of  $\text{Ag}^+$  and  $\text{Hg}^{2+}$  binding with PT18C6. These curves could be considered as *microscopic interaction energy curves*.

### Conclusions

By the replacement of the S of  $\text{T}_218\text{C}_6$  by pyridone, a large enhancement of selectivity for  $\text{Ag}^+$  over  $\text{Hg}^{2+}$  and  $\text{Pb}^{2+}$  was found. A dramatic decrease of the interaction of the pyridone half of the ligand with  $\text{Hg}^{2+}$  was found with use of  $^{13}\text{C}$  NMR measurements which results in a dramatic decrease in the  $\log K$  value for the interaction. Meanwhile, an increase of the interaction of  $\text{Ag}^+$  with the pyridone half of the ligand was found which results in a modest increase in  $\log K$  for this interaction. The microscopic information of  $T_1$  and  $\delta$  provides a solid basis for the explanation of the macroscopic selectivity of PT18C6 for  $\text{Ag}^+$  over  $\text{Hg}^{2+}$ . The reversal of the normal selectivity order of  $\text{Hg}^{2+}$  over  $\text{Ag}^+$  can be attributed to the combination of the special affinity of pyridone nitrogen for  $\text{Ag}^+$  and the inclusion of  $\text{Ag}^+$  in the macrocycle cavity. Possible coordination patterns of an inclusion type of  $\text{Ag}^+$ -PT18C6 and a perching type of  $\text{Hg}^{2+}$ -PT18C6 are illustrated in Figure 4. These structures with minimized energy are derived from molecular mechanics calculations.<sup>17</sup> A prediction which results from this study is that a dipyridon-18C6 may result in an even larger selectivity toward  $\text{Ag}^+$  over  $\text{Hg}^{2+}$  than PT18C6. It is intended to test this prediction.

**Acknowledgment.** We appreciate the financial support from the Department of Energy, Office of Basic Energy Sciences, Grant No. DE-FG02-86ER13463. We thank Visiting Professor Du Li (Lanzhou University, PRC) and Professor Noel Owen (BYU) for helpful discussions on  $T_1$  measurements.

(15) Rahman, Atta-ur *Nuclear Magnetic Resonance*; Springer-Verlag: New York, 1986; pp 126-130.

(16) Echegoyen, L.; Kaifer, A.; Durst, H.; Schultz, R. A.; Dishong, D. M.; Gpli, D. M.; Gokel, G. W. *J. Am. Chem. Soc.* **1984**, *106*, 5100-5103.

(17) PCMODEL, available from Serena Software, Box 3076, Bloomington, IN 47402-3076.